

1 stepped pressure equilibrium code : future

Contents

1	stepped pressure equilibrium code : future	1
1.1	outline	1
2	finite-pressure plasma surrounded by a vacuum with a chaotic separatrix	2
2.1	derive equations for Beltrami field with non-zero normal field at outer interface	2
2.2	construct ‘toy-model’ of plasma-vacuum equilibrium	2
2.3	illustrate hetero-clinic tangle	2
2.4	illustrate cantori in vacuum region	3
2.5	solve the anisotropic heat diffusion equation in chaotic vacuum region	3
2.6	implementation of more realistic physics model in ‘vacuum’ region	3
2.7	initial results	3

1.1 outline

1. Describes ongoing and/or planned research activities.

2 finite-pressure plasma surrounded by a vacuum with a chaotic separatrix

2.1 derive equations for Beltrami field with non-zero normal field at outer interface

1. Extremize the energy functional

$$F \equiv \int_{\mathcal{V}} \frac{B^2}{2} dv - \frac{\mu}{2} \int_{\mathcal{V}} \mathbf{A} \cdot \mathbf{B} dv, \quad (1)$$

with respect to variations, $\delta\mathbf{A}$, in the vector potential, $\mathbf{B} = \nabla \times \mathbf{A}$, in an annular volume bounded by an inner toroidal surface, \mathcal{I}_{N-1} and an outer toroidal surface, \mathcal{I}_N , under the boundary conditions $\mathbf{B} \cdot \mathbf{n} = 0$ on \mathcal{I}_{N-1} and $\mathbf{B} \cdot \mathbf{n} = b$ on \mathcal{I}_N , where b is a user supplied function. The ‘toroidal’ and ‘poloidal’ fluxes are also to be constrained.

2. The first variation in F is

$$\delta F = \int_{\mathcal{V}} \delta\mathbf{A} \cdot (\nabla \times \mathbf{B} - \mu\mathbf{B}) dv + \int_{\partial\mathcal{V}} \delta\mathbf{A} \times \mathbf{B} \cdot d\mathbf{s} - \frac{\mu}{2} \int_{\partial\mathcal{V}} \delta\mathbf{A} \times \mathbf{A} \cdot d\mathbf{s}. \quad (2)$$

3. If the outer boundary is not a flux surface, how are the toroidal and poloidal fluxes defined?
4. Are there any constraints on $b \equiv \mathbf{B} \cdot \mathbf{n}$? Note that $0 = \int \nabla \cdot \mathbf{B} dv = \int \mathbf{B} \cdot d\mathbf{s} = \int \mathbf{B} \cdot \nabla s \sqrt{g} d\theta d\zeta$.
5. Constrain the variations in $\delta\mathbf{A}$ to (i) constrain the toroidal and poloidal fluxes, and (ii) preserve the boundary conditions on $\mathbf{B} \cdot \mathbf{n}$; and simplify the surface integrals.
6. Does this theoretical approach lead to a simple, robust method for constructing Beltrami fields, $\nabla \times \mathbf{B} = \mu\mathbf{B}$?
7. For $\mu = 0$, this method should produce vacuum fields. How does this method compare (in terms of accuracy, robustness and speed) to alternative methods of solving Laplace’s equation?
8. Implement this method into SPEC and perform convergence tests that demonstrate that the solutions are accurately being computed. (This has mostly been completed; see figures below.)

2.2 construct ‘toy-model’ of plasma-vacuum equilibrium

1. Provide an outer boundary to SPEC that approximates the size and shape of the DIII-D inner wall, for example.
2. Modify SPEC so that the Beltrami field in the outermost volume is constrained to be a vacuum field.
3. Determine normal field on outer boundary that results in a separatrix in outermost volume, and adjust this normal field so that the plasma-vacuum equilibrium is surrounded by a DIII-D-like separatrix.
4. Apply a perturbation to the normal field so that the region near the separatrix becomes chaotic.
5. If the external field is provided, can an application of the virtual casing method [1] be used to construct a true ‘free-boundary’ equilibrium?
6. What is the primary effect of the perturbation field. Is it to ergodize the vacuum region or to force islands in the plasma interior?
7. To what extent do the ideal interfaces (required to support pressure gradients) create a shielding effect?

2.3 illustrate hetero-clinic tangle

1. By locating fixed points, trace out the unstable manifold [2] associated with the chaotic separatrix.
2. Examine the effect of the unstable manifold on the plasma-vacuum interface.
3. Is there a simple characterization of the unstable manifold (e.g. area and location of primary ‘lobes’) that is relevant for understanding the deformation of the plasma-vacuum interface?
4. Vary the rotational-transform, ι , on the plasma-vacuum interface. Are there certain ‘resonant’ values of the edge- ι that, for a given perturbed normal field result in a ‘large’ unstable manifold and ergodization of the vacuum region?

2.4 illustrate cantori in vacuum region

1. By constructing [3] minimizing, high-order, periodic field lines, illustrate the most effective cantori in the vacuum region.
2. Show how the cantori and the unstable manifold interact.
3. Compute field-line flux through cantori. Show how the field line flux varies with edge- ϵ .

2.5 solve the anisotropic heat diffusion equation in chaotic vacuum region

1. The numerical routines for solving the anisotropic heat diffusion equation have already been constructed [4] and should be easily implemented into SPEC.
2. Compute heat flux on wall.
3. Can any qualitative comparisons with experimental results be derived (e.g. heat flux on divertor plates).
4. If an appropriate free-boundary problem is solved, can quantitative comparisons and/or predictions be made?

2.6 implementation of more realistic physics model in ‘vacuum’ region

1. Perhaps the assumption that the plasma is surrounded by a vacuum is too simple, and perhaps instead there are plasma currents and various non-ideal effects that are important in this region.
2. Derive a tractable set of equations that capture the relevant physical effects in this region.
3. Implement a numerical solution method.

2.7 initial results

1. Much of the numerical work has already been done, and an example calculation is shown in Fig.1.
2. Fig.2 confirms that the vacuum field with non-zero normal field in the outermost boundary is converged with respect to radial resolution.
3. Fig.3 confirms that the equilibrium geometry is converged with respect to the Fourier resolution.

future.h last modified on 2012-10-22 ;

- [1] V. D. Shafranov and L. E. Zakharov. Use of the virtual-casing principle in calculating the containing magnetic field in toroidal plasma systems. *Nucl. Fus.*, 12:599, 1972.
- [2] R. K.W. Roeder, B. I. Rapoport, and T. E. Evans. Explicit calculations of homoclinic tangles in tokamaks. *Phys. Plasmas*, 10(9):3796, 2003.
- [3] S. R. Hudson. Calculation of cantori for Hamiltonian flows. *Phys. Rev. E.*, 74:056203, 2006.
- [4] S. R. Hudson and J. Breslau. Temperature contours and ghost-surfaces for chaotic magnetic fields. *Phys. Rev. Lett.*, 100(9):095001, 2008.

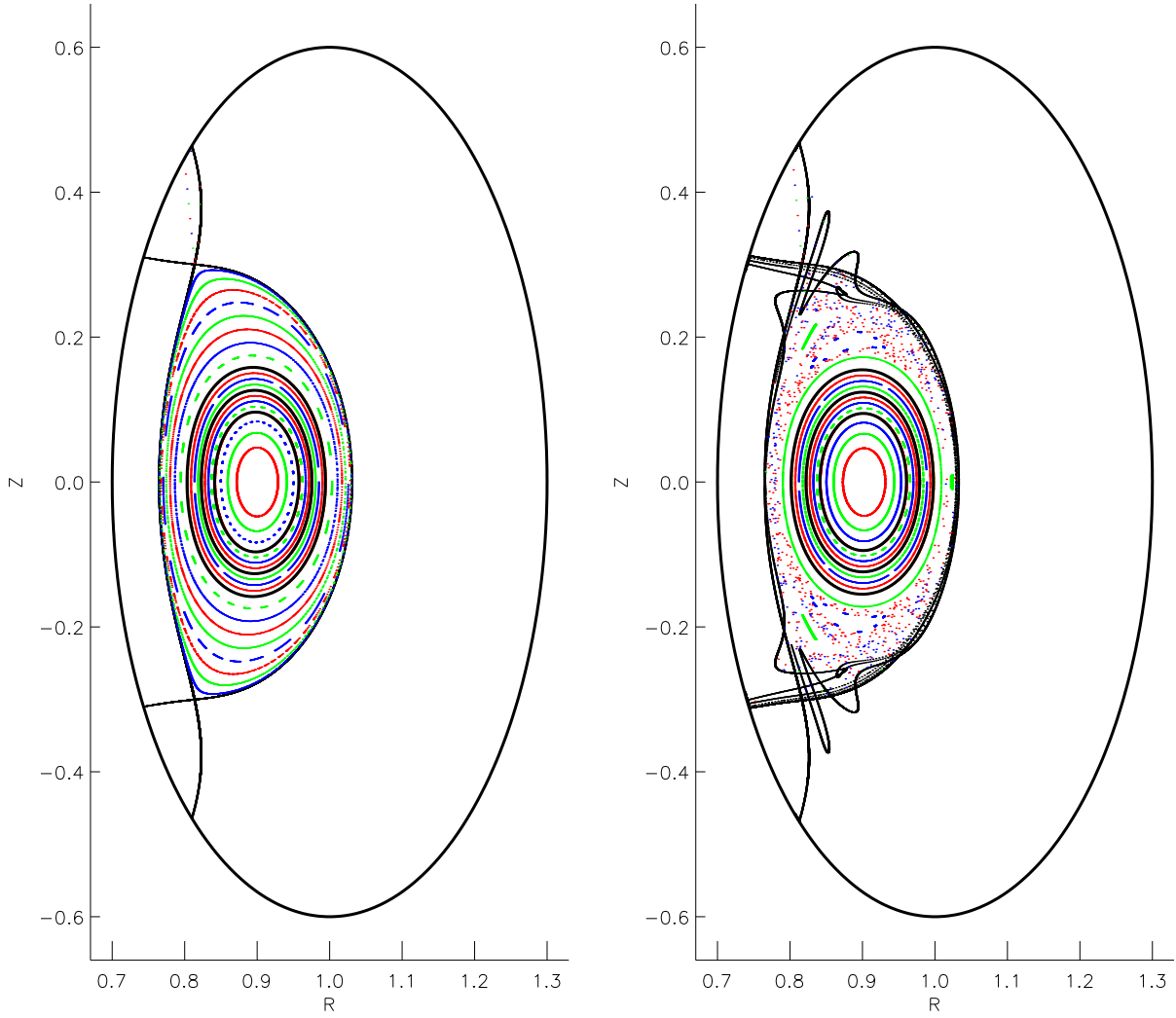


Figure 1: Finite pressure plasma equilibrium surrounded by a vacuum field with separatrix: the outermost boundary is considered to be the ‘wall’ of an experimental device on which a non-zero normal field is imposed that results in separatrix; in the outermost volume, the field satisfies $\nabla \times \mathbf{B} = 0$; in the other volumes the field satisfies $\nabla \times \mathbf{B} = \mu \mathbf{B}$; there are several interior interfaces (shown with thick, black lines) which support pressure discontinuities; the left figure shows an axisymmetric calculation, and the right figure includes a small non-axisymmetric normal field at the wall which results in an ergodic field.

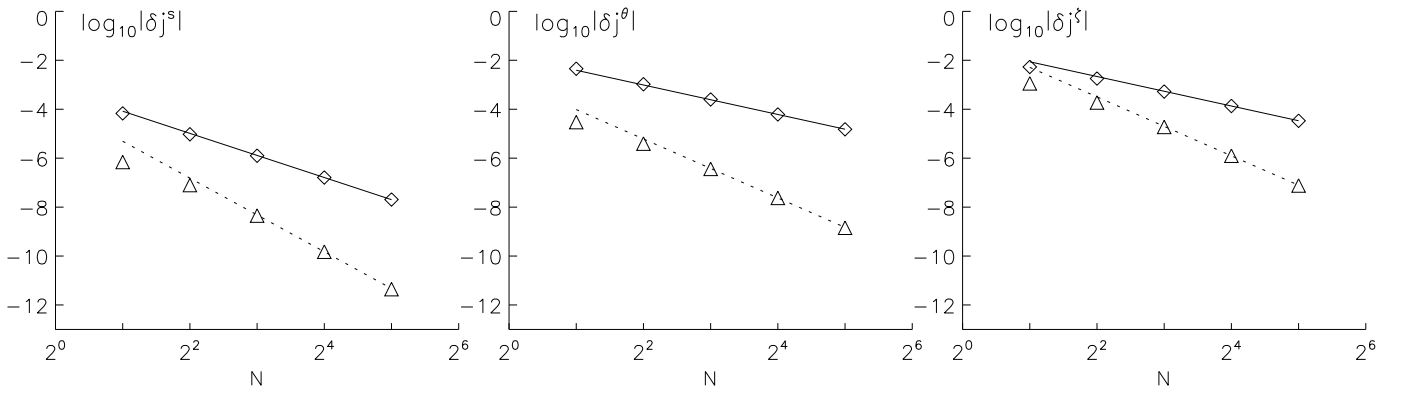


Figure 2: Radial resolution convergence study: the resolution of the radial sub-grid in the outermost volume, the vacuum region with non-zero normal field at the wall, is increased and the error in $\nabla \times \mathbf{B} = 0$ is computed; the expected error scaling for piecewise cubic and piecewise quintic radial basis functions are obtained.

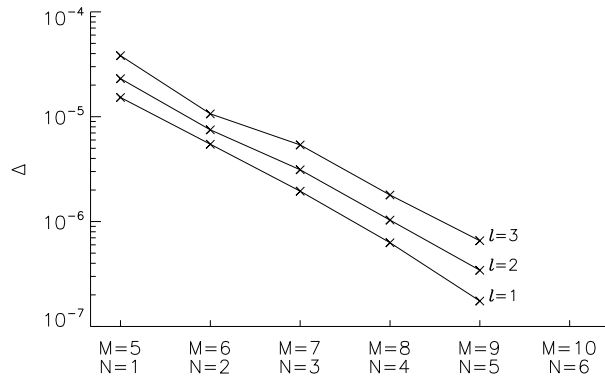


Figure 3: Fourier resolution convergence study: the quantity Δ measures the difference between the geometry of a finite Fourier resolution SPEC equilibrium and a reference, high resolution SPEC equilibrium.